NON-MAXWELLIAN VELOCITY DISTRIBUTION FUNCTIONS ASSOCIATED WITH STEEP TEMPERATURE GRADIENTS IN THE SOLAR TRANSITION REGION

Paper II. The Effect of Non-Maxwellian Electron Distribution Functions on Ionization Equilibrium Calculations for Carbon, Nitrogen and Oxygen

Robert Roussel-Dupré*

Department of Astro-Geophysics
University of Colorado
Boulder, Colo. 80309, U.S.A.

*Presently at University of Hawaii, Institute for Astronomy, 2680 Woodlawn Drive, Honolulu, Hawaii 96822, U.S.A.

(NASA-CR-162695) NON-MAXWELLIAN VELOCITY DISTRIBUTION FUNCTIONS ASSOCIATED WITH STEEP TEMPERATURE GRADIENTS IN THE SOLAR TRANSITION REGION. PAPER 2: THE EFFECT OF NON-MAXWELLIAN ELECTRON DISTRIBUTION (Hawaii G3/72 11677

N80-16852

Unclas

ABSTRACT

Non-Maxwellian electron velocity distribution functions, computed for Dupree's 1972 model of the solar transition region in a previous paper, are used to calculate ionization rates for ions of carbon, nitrogen, and oxygen. Ionization equilibrium populations for these ions are then computed and compared with similar calculations assuming Maxwellian distribution functions for the electrons. The results show that the ion populations change (compared to the values computed with a Maxwellian) in some cases by several orders of magnitude depending on the ion and its temperature of formation.

1. INTRODUCTION

The ionization equilibrium calculations found in the literature, to date, make use of various theoretical and semi-empirical cross-sections to compute ionization and recombination rates (Allen and Dupree, 1969; Jordan, 1969; Summers, 1974; Jacobs et al., 1977a and b). All of these studies, however, assume that the velocity distribution function for ionizing electrons is a Maxwellian.

If the ionization energy, χ, is large compared to the local electron thermal energy, then it is important that we have an accurate description of the tail of the electron distribution function in order to compute the ionization rate, q_i. In Table I we list the ionization energies for various ions found in the transition region, along with the temperature (T_{max}) at which the ion has its maximum population relative to n_E - based on Jordan's (1969) results - and the ionization energy normalized to kT_{max}. We find that χ/kT_{max} ranges from 5-15. Roussel-Dupré (1980, hereafter Paper I) showed that the electron distribution function is non-Maxwellian for energies around 6 kT, where $T = 10^{5.2}$ K, and we may conclude therefore that present ionization equilibrium calculations may need serious revision, especially for ions formed primarily in the region from 10^5 - 10^6 K. We also note that an increase in the population of the tail of the distribution function will increase the ionization rates, since a threshold energy is involved. On the other hand, the cross-sections for recombination decreases with energy and no threshold is required; therefore, we do not expect recombination rates to be affected.

In this paper, we use the electron distribution functions, computed in Paper I for Dupree's (1972) model of the transition region, to compute ionization rates for ions of carbon, nitrogen and oxygen. We then

recompute the ionization equilibrium populations for these various ions and compare our results with calculations for a Maxwellian distribution.

2. CORRECTED IONIZATION RATES

For our purposes, we chose to work with the semi-empirical cross-section, given by Allen (1973), for direct ionization from the ground state. This cross-section is given by,

$$Q_i(\varepsilon) = 3.59 \times 10^{-14} \sum \frac{\delta(n,\ell)}{\chi_{ev}^2(n,\ell)} \frac{\chi(n,\ell)}{\varepsilon} \left(1 - \frac{\chi(n,\ell)}{\varepsilon}\right) \text{cm}^2 \qquad (1)$$

where $\delta(n,\ell)$ is the number of bound electrons with quantum numbers n and ℓ, $\chi_{ev}(n,\ell)$ is the ionization potential in electron volts and ε is the electron energy. To compute the auto-ionization rates, we used the cross-section for excitation from state i to state j, given by,

$$Q_{ij}(\varepsilon) = \frac{3.792 \times 10^{-26}}{\chi_{ev}} f_{ij} \bar{g} \frac{1}{\varepsilon} \qquad (2)$$

where f_{ij} is the oscillator strength and $\bar{g}$ is a Gaunt factor (~ 0.2). These cross-sections agree with experimental measurements to within a factor of 2 (See Elwert 1952). Although there are more accurate experimental results available for specific ions, we are only interested in estimating the effect of the electron tail on ionization equilibrium calculations for the ionization stages of several elements, and approximate cross-sections are accurate enough for this purpose.

In order to evaluate the effect of the tail of the electron distribution function on ionization rates, we computed the ratio of these rates, calculated with the non-Maxwellian distribution function given by equation (22) of Paper I, to the corresponding rates calculated

assuming a Maxwellian distribution function. This ratio, for direct ionization from the ground state is given as a function of $I(=\chi/kT)$ and u_c, the critical speed above which deviations from Maxwellian are large by,

$$R_i^{>}(I,u_c^2) = \frac{1}{2} + \left[\frac{u_c}{4} \left[3 + u_c^2 \exp(-u_c^2) \left(G(I,u_c^2) - \exp(I)/I\right)\right] \right.$$

$$\times \left[\sqrt{\pi}\, erfc(\sqrt{I}) \left(1 + 2I\right) - 2I \exp(-I)\right]$$

$$\left. + 7/4 \left(\frac{u_c^2}{I}\right)^{9/7} E_{10}\left(I^{1/7}\left(u_c^2\right)^{6/7}\right)\right] \Big/ \left(\exp(-I) - I\, E_1(I)\right)$$

$$I \geq u_c^2 \qquad (3)$$

$$R_i^{<}(I,u_c^2) = 1 + \left[\left(\frac{1+2I}{2}\right) \left[\sqrt{\pi}\, u_c\, erfc(u_c) - \exp(u_c^2)\right] \right.$$

$$\left. + I\, E_1\left(u_c^2\right)/2 + 7/4\, E_{10}\left(u_c^2\right)\right] \Big/ \left[\exp(-I) - I\, E_1(I)\right]$$

$$I \leq u_c^2 \qquad (4)$$

For auto-ionization we find,

$$R_a^{>}(I,u_c^2) = \frac{1}{2} + \left[\frac{u_c}{4} \left[3 + u_c^2 \exp(-u_c^2)\left(G(I,U_c^2) - \exp(I)/I\right)\right] \times \left[\sqrt{\pi}\; erfc\left(\sqrt{I}\right)\right] \right.$$

$$\left. + 7/4 \left(u_c^2/I\right)^{9/7} E_{10}\left(I^{1/7}\left(u_c^2\right)^{6/7}\right)\right] \exp(I)$$

$$I \geq u_c^2 \qquad (5)$$

$$R_a^{<}(I,u_c^2) = 1 + \left[\frac{1}{2} \left[\sqrt{\pi}\, u_c\, erfc\,(u_c) - \exp(-u_c^2)\right] + 7/4\, E_{10}(u_c^2)\right] \exp(I)$$

$$I \leq u_c^2 \qquad (6)$$

where $erfc(x)$ is the complementary error function; $E_{10}(x)$ and $E_1(x)$ are the tenth and first exponential integrals respectively and $G(I,u_c^2)$ is defined by,

$$G(I,u_c^2) = \int_1^{I/u_c^2} \frac{\exp(u_c^2 x)}{x} \, dx \quad .$$

By simple substitution, we can show that equations (3) - (6) satisfy the conditions.

$$R_i^<(I,u_c^2) \to 1 \text{ as } u_c \to \infty$$

$$R_i^>(I,I) \doteq R_i^< (I,I)$$

$$R_a^<(I,u_c^2) \to 1 \text{ as } u_c \to \infty$$

$$R_a^>(I,I) = R_a^<(I,I) \quad .$$

As a typical example, we list, in Table II, values of R_i and R_a for the carbon IV ion, as a function of temperature and the critical speeds, u_c, computed from Dupree's model in Paper I. The non-Maxwellian tail leads to ionization rates which can be as much as a factor of ten larger than those computed assuming a Maxwellian. In addition, since radio observations predict a lower pressure (or density) by a factor of three or more for the transition region than EUV observations (cf., Dulk et al., 1977), we have also listed these ratios for Dupree's model with the pressure decreased by a factor of three. The latter results yield larger ratios simply because the critical speeds are decreased, extending the tail over a larger range in velocity space and further increasing the population of high energy electrons relative to a Maxwellian.

3. IONIZATION EQUILIBRIUM CALCULATIONS

We are interested in computing the effect of these higher ionization rates on the relative populations of the various ionization stages of a given element in ionization equilibrium in the transition region. The relative population of two neighboring ionization stages for a given element is computed directly from

$$\frac{n(x^{+m+1})}{n(x^{+m})} = \frac{\sum_i q_i(x^{+m})}{\sum_r \alpha_r(x^{+m})} \qquad (7)$$

where $q_i(x^{+m})$ represents the ionization rate for an ion in ionization stage m by a process i, $\alpha_r(x^{+m})$ represents the recombination rate for an ion x^{+m} by a process r and the sums i and r are over all ionization and recombination processes, respectively.

In our analysis, we considered direct ionization from the ground state, auto-ionization, radiative recombination and di-electronic recombination to be the most important ionization and recombination processes for ions in the transition region. The di-electronic recombination rates used in our computations were used in the calculations of Allen and Dupree (1969) and provided by Joselyn. The states which auto-ionize for a given ion were obtained by means of a scheme described by Jordan (1969). The ionization rate from the ground state was computed in the manner described in the previous section and the radiative recombination rates were computed directly from equation (2-13) of Allen and Dupree (1969), assuming a Maxwellian distribution function; however, this is a good approximation since the tail only affects recombination rates by a few percent at most.

Finally, we computed the fractional ion populations (N_i/N_e) for the

various ionization stages of carbon, nitrogen and oxygen in ionization equilibrium. The results, using Dupree's model to compute u_c, are presented in Figures 1-3; while the results, using Dupree's model with the pressure reduced by a factor of three to compute u_c, are shown in Figures 4-6. In each of these figures, the solid curves are based on the assumption that the distribution functions are Maxwellian. The dashed curves take into account the effect of the electron tail. In the region where the temperature gradient is steepest, we find that the lower ionization stages of all these elements are depleted by the increased ionization caused by the tail. The higher ionization stages have increased populations throughout the upper half of the transition region suggesting that ions, thought to form only in the corona, can have substantial populations in the transition region. The changes in population can be many orders of magnitude for Dupree's model and are even higher when the pressure is lowered by a factor of three.

As pointed out in Paper I, it is impossible to pinpoint the exact value of the critical energy. As a result, we decided to present calculations for a minimum and maximum critical energy. The results presented above correspond to the minimum value. In Figure 7, we present ionization equilibrium populations for carbon in the same format described above, computed with the maximum critical energy. We find that these results show no apparent difference from those obtained with a Maxwellian for the majority of ionization stages of carbon except C VI which has a large ionization potential.

We can conclude that the effect of the high energy tails on ionization equilibrium is sensitive to the location of the tail. This means that the exact magnitude of this effect cannot be pinpointed by our method of

approximation and that this problem will remain unresolved until detailed calculations, which would involve a solution of the Boltzmann-Fokker-Planck equation, are presented. However, we have argued in Paper I that the minimum critical energies used in our calculations represent a good approximation for the location of the tail.

4. SUMMARY

The effect of the high energy tails on ionization equilibrium calculations is summarized in Figures 1 - 7. We found that the ion populations change (compared to the values computed with a Maxwellian) by as much as several orders of magnitude depending on the ion and its temperature of formation. We also found, however, that these results are sensitive to the location of the high energy tail in velocity space and that detailed solutions of the Boltzmann-Fokker-Planck equation are necessary to determine the exact magnitude of these effects. However, arguments presented in Paper I suggest that the minimum critical energies represent a good approximation for the locations of the tails so that the results obtained with these critical energies are reasonable approximations for the changes in ion populations.

The effect of the high energy tails on ionization equilibrium calculations is significant. This result has serious implications for the interpretation of EUV line profiles to yield models for the transition region. The high energy tails affect the collisional excitation rates (not computed here), ion populations and the temperature range over which ions form. Both excitation rates and ion populations enter into line intensity calculations. We can conclude that our results may significantly change the models which we compute from EUV line observations. However, since detailed calculations which include the effects of high energy tails on computed line profiles have not been presented, it is

difficult to conclude, at this point, exactly what changes will result in present models. Calculation of a self-consistent model, for the transition region, which reproduces EUV line observations is a topic for future research.

Finally, we note that the effect of magnetic fields at an angle to the temperature gradient was not included in our calculations. Considering the multitude of magnetic field configurations observed on the solar surface, a study of transport processes in the presence of magnetic fields and large temperature gradients is essential and remains a subject for future research. In addition, we mention that the analyses presented here and in Paper I are not limited to the transition region but are applicable to any plasma where steep gradients are encountered.

ACKNOWLEDGEMENTS

I would like to thank Dr. D. E. Billings for suggesting this research and for his constant support and encouragement. Special thanks are extended to Dr. Dean Smith and Dr. John Jefferies for many helpful discussions. The financial support for this research was provided over several years by a number of NSF contracts: ATM 78-22202 and GA-31477. In addition, NASA contract NAS-5-22409 funded through the Laboratory for Atmospheric and Space Physics (LASP) provided support for an interim period of two months. This paper was prepared at the Institute for Astronomy, University of Hawaii, support provided by NASA Grant NSG 7536.

REFERENCES

Allen, C. W.: 1973, Astrophysical Quantities, 3rd ed., The Athlone Press.

Allen, J. W. and Dupree, A. K.: 1969, Ap. J., 155, No. 1, Part 1, 27.

Dulk, G. A., Sheridan, K. V., Smerd, S. F., and Withbroe, G. L.: 1977, Solar Phys. 52, 349.

Dupree, A. K.: 1972, Ap. J., 178, 527.

Elwert, G.: 1952, Z. Naturf., 7a, 703.

Jacobs, V. L., Davis, J., Kepple, P. C., and Blaha, M.: 1977a, Ap. J. 211, 605.

Jacobs, V. L., Davis, J., Kepple, P. C., and Blaha, M.: 1977b, Ap. J. 215, 690.

Jordan, C.: 1969, Mon. Not. R. Astr. Soc., 142, 501.

Roussel-Dupré, R. A.: 1980, submitted to Solar Phys.

Summers, H. P.: 1974, Appleton Laboratory Internal Memo 367, Culham Laboratory, Abingdon, Oxon, England.

TABLE I

RATIOS OF IONIZATION ENERGIES TO LOCAL TEMPERATURES OF FORMATION FOR SEVERAL IONS

Ion	Ionization Energy x (ev)	Log T_{max}	x/kT_{max}
C II	24.4	4.30	1.42(1)
C III	47.9	4.85	7.84
N II	29.6	4.40	1.37(1)
N III	47.5	4.95	6.17
N V	98.9	5.30	5.75
O III	54.9	4.90	8.01
O IV	77.4	5.25	5.05
O V	114.0	5.40	5.26
O VI	138.0	5.50	5.06

TABLE II

RATIOS OF CIV IONIZATION RATES COMPUTED WITH A TAIL TO THOSE COMPUTED WITH A MAXWELLIAN

Log T	R_{i/R_i}* $P = P_o$	R_{a/R_a}* $P = P_o$	R_{i/R_i}* $P = P_o/3$	R_{a/R_a}* $P = P_o/3$
4.7	1.01	1.00	3.32	1.58(1)
4.8	3.13	1.26(1)	3.03(1)	3.08(1)
5.0	3.64	8.87	1.09(1)	1.39(1)
5.2	1.80	5.42	2.99	6.02
5.4	1.06	1.01	1.31	1.05
5.6	1.01	1.00	1.04	1.01
5.8	1.00	1.00	1.01	1.00
6.0	1.00	1.00	1.00	1.00
6.2	1.00	1.00	1.00	1.00

FIGURE CAPTIONS

Figures 1-3 Fractional ion populations for the ionization stages of carbon, nitrogen and oxygen (Dupree's model).

Figures 4-6 Fractional ion populations for the ionization stages of carbon, nitrogen and oxygen (Dupree's model with pressure reduced by a factor of three).

Figure 7 Fractional ion populations for the ionization stages of carbon ($U_c^2 = (0.4)^{\frac{1}{2}}(U_c^2)_D$).

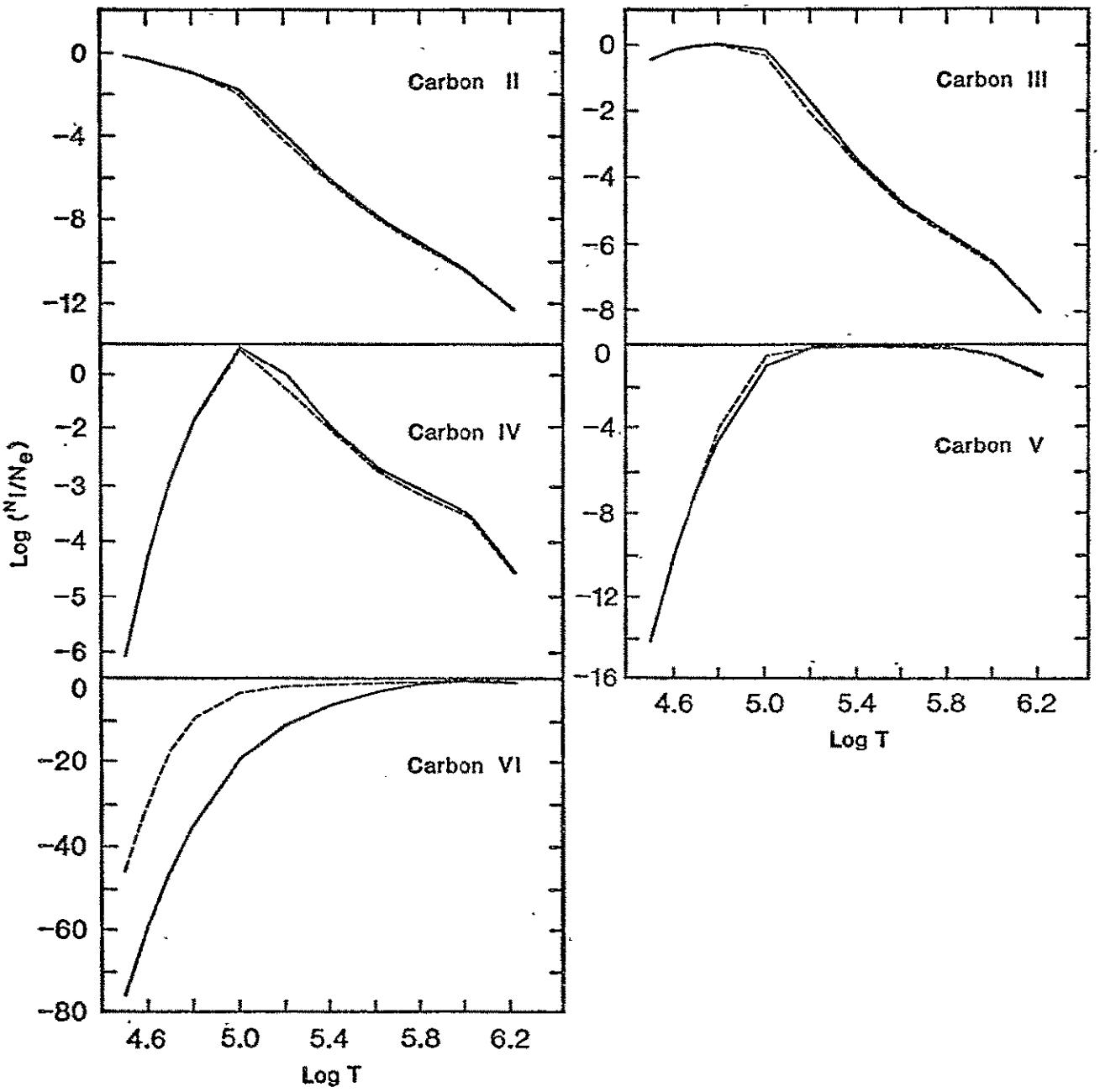
Carbon II
Carbon III
Carbon IV
Carbon V
Carbon VI
Log (N_I/N_e)
Log T
Log T

Figure 1

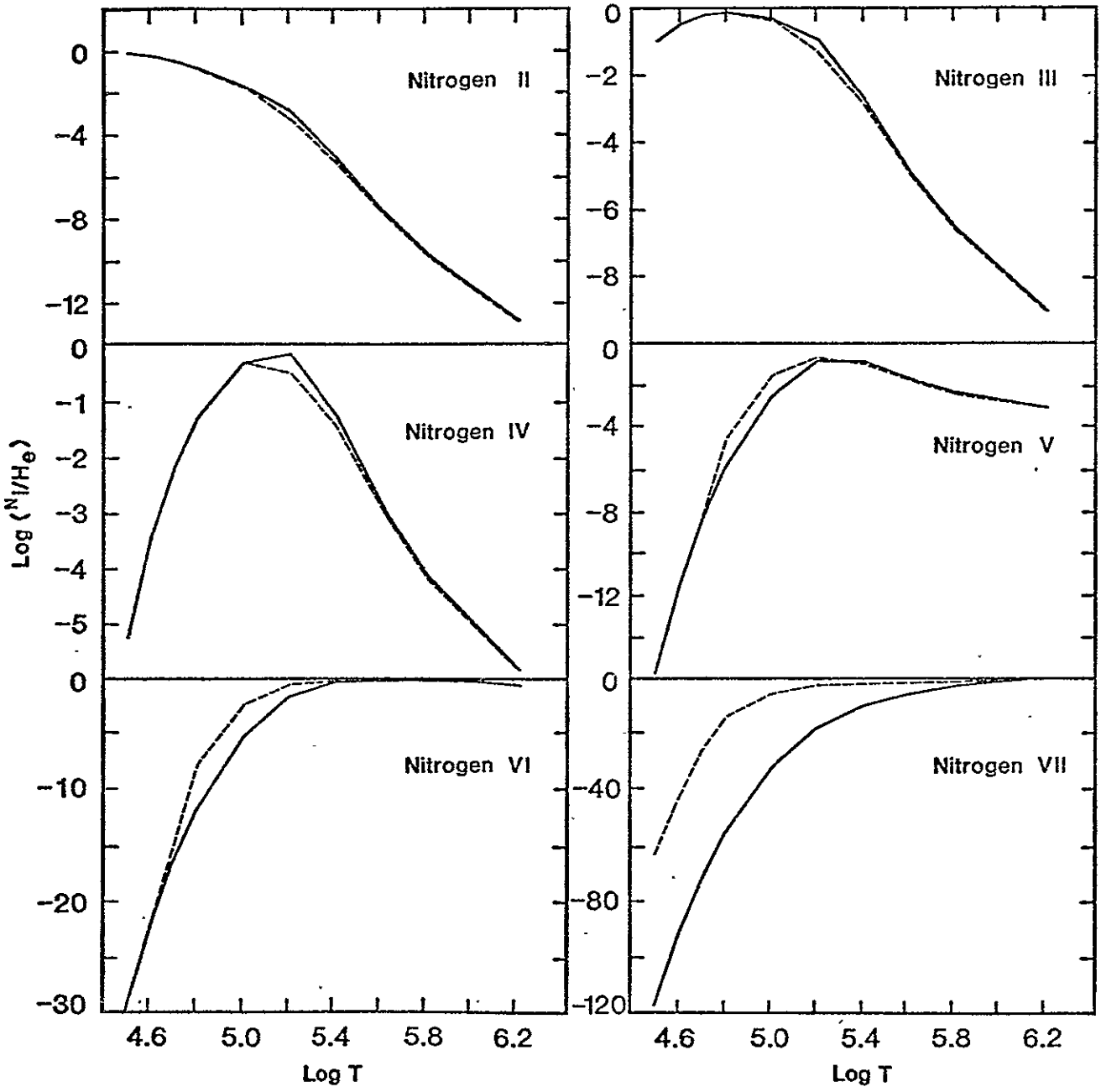
Nitrogen II
Nitrogen III
Nitrogen IV
Nitrogen V
Nitrogen VI
Nitrogen VII
Log (N_I/H_e)
Log T
Log T
0
-4
-8
-12
-2
-6
-1
-3
-5
-10
-20
-30
-40
-80
-120
4.6
5.0
5.4
5.8
6.2

Figure 2

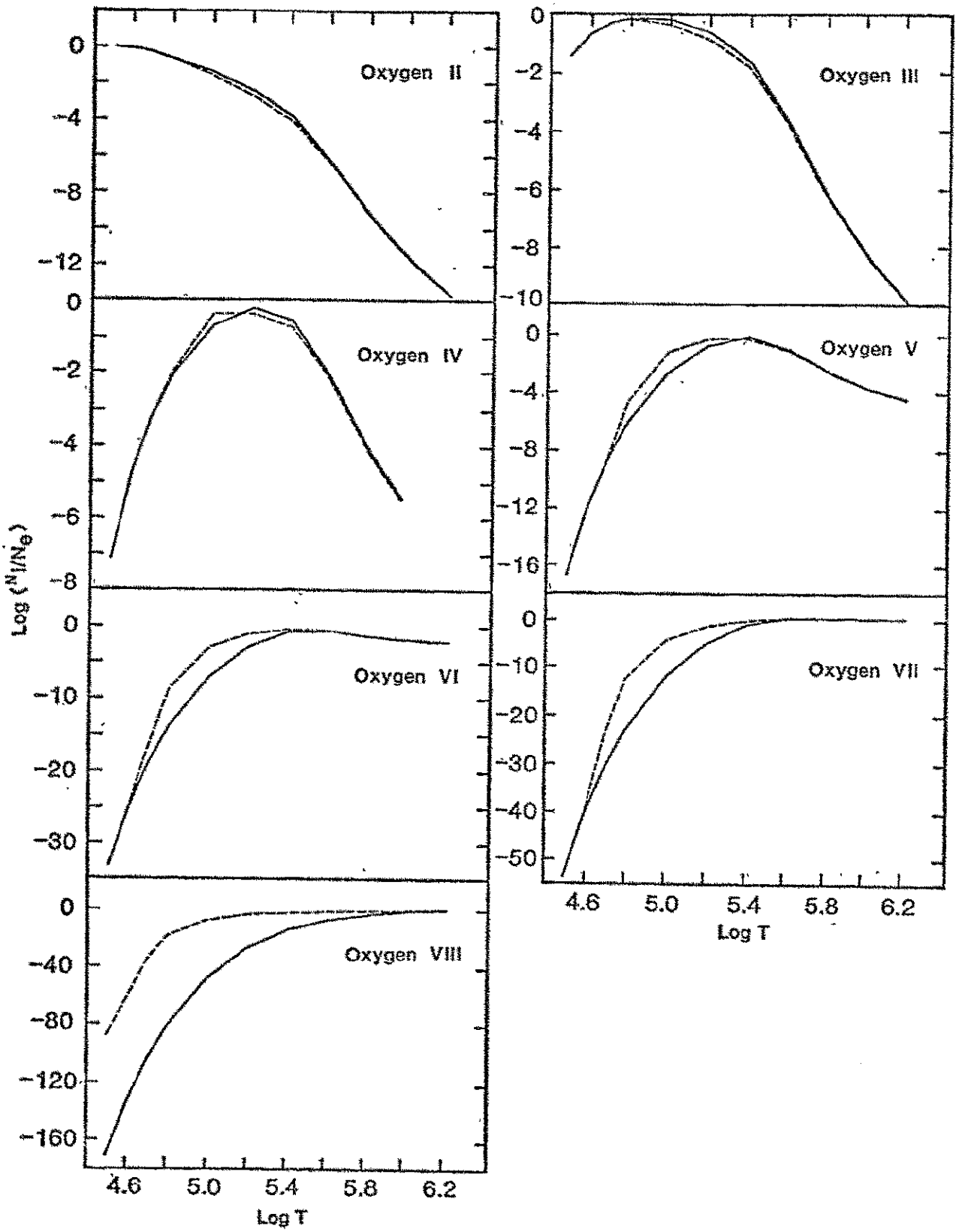
Oxygen II
Oxygen III
Oxygen IV
Oxygen V
Oxygen VI
Oxygen VII
Oxygen VIII
Log (N_I/N_e)
Log T
4.6
5.0
5.4
5.8
6.2

Figure 3

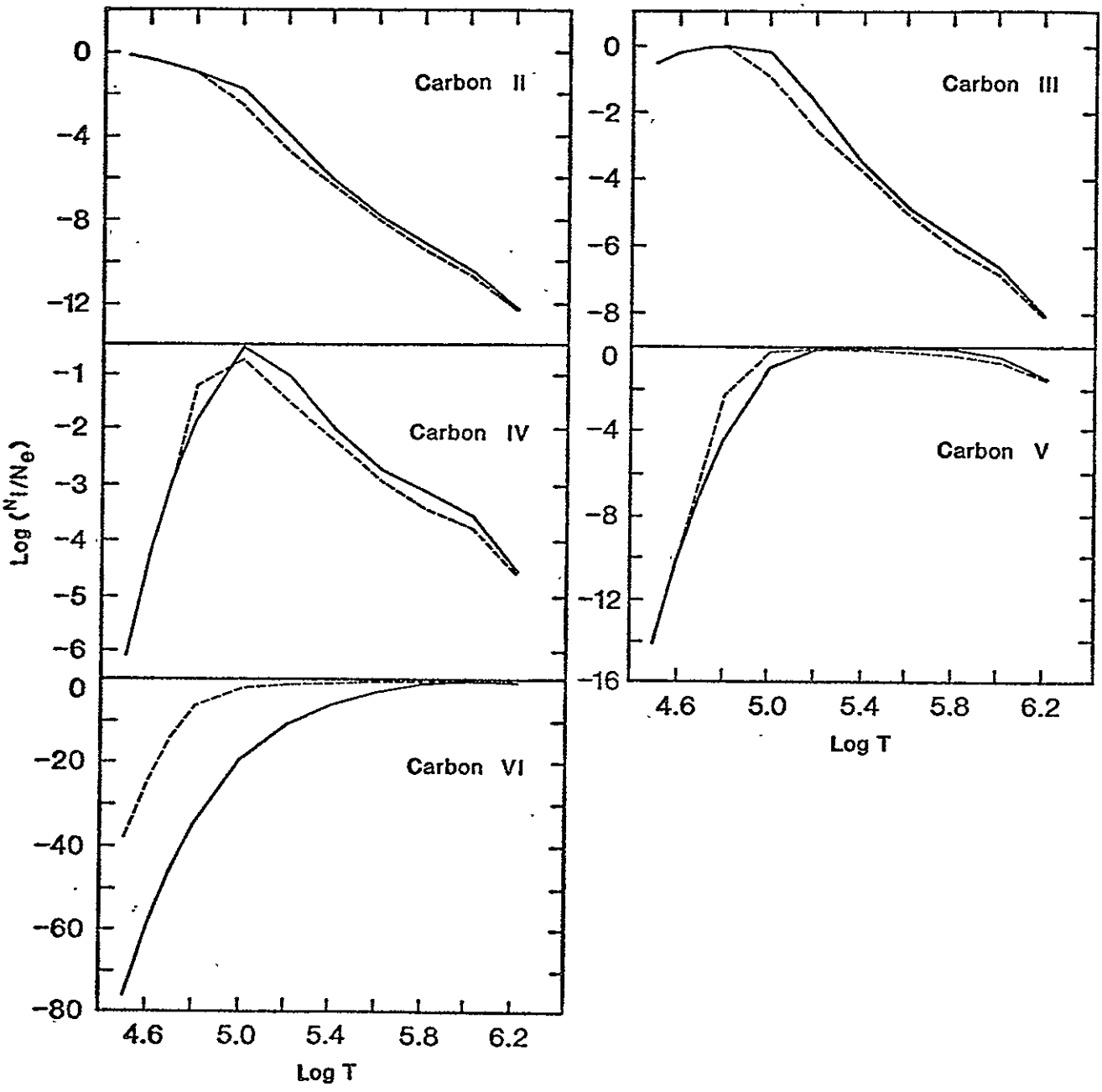
Carbon II
Carbon III
Carbon IV
Carbon V
Carbon VI
Log (N_i/N_e)
Log T
4.6
5.0
5.4
5.8
6.2

Figure 4

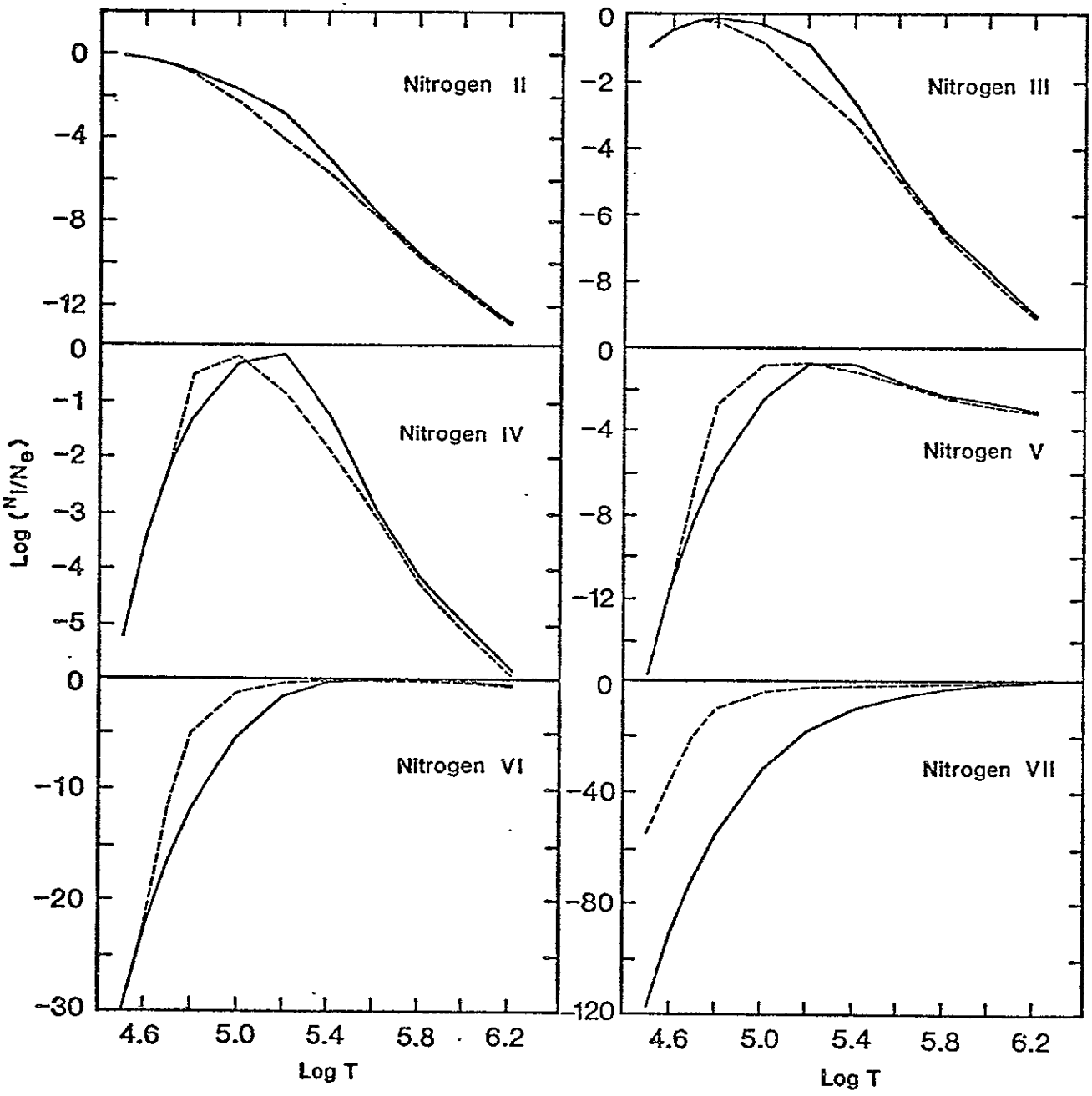
Nitrogen II
Nitrogen III
Nitrogen IV
Nitrogen V
Nitrogen VI
Nitrogen VII
Log (N_I/N_e)
Log T
4.6
5.0
5.4
5.8
6.2

Figure 5

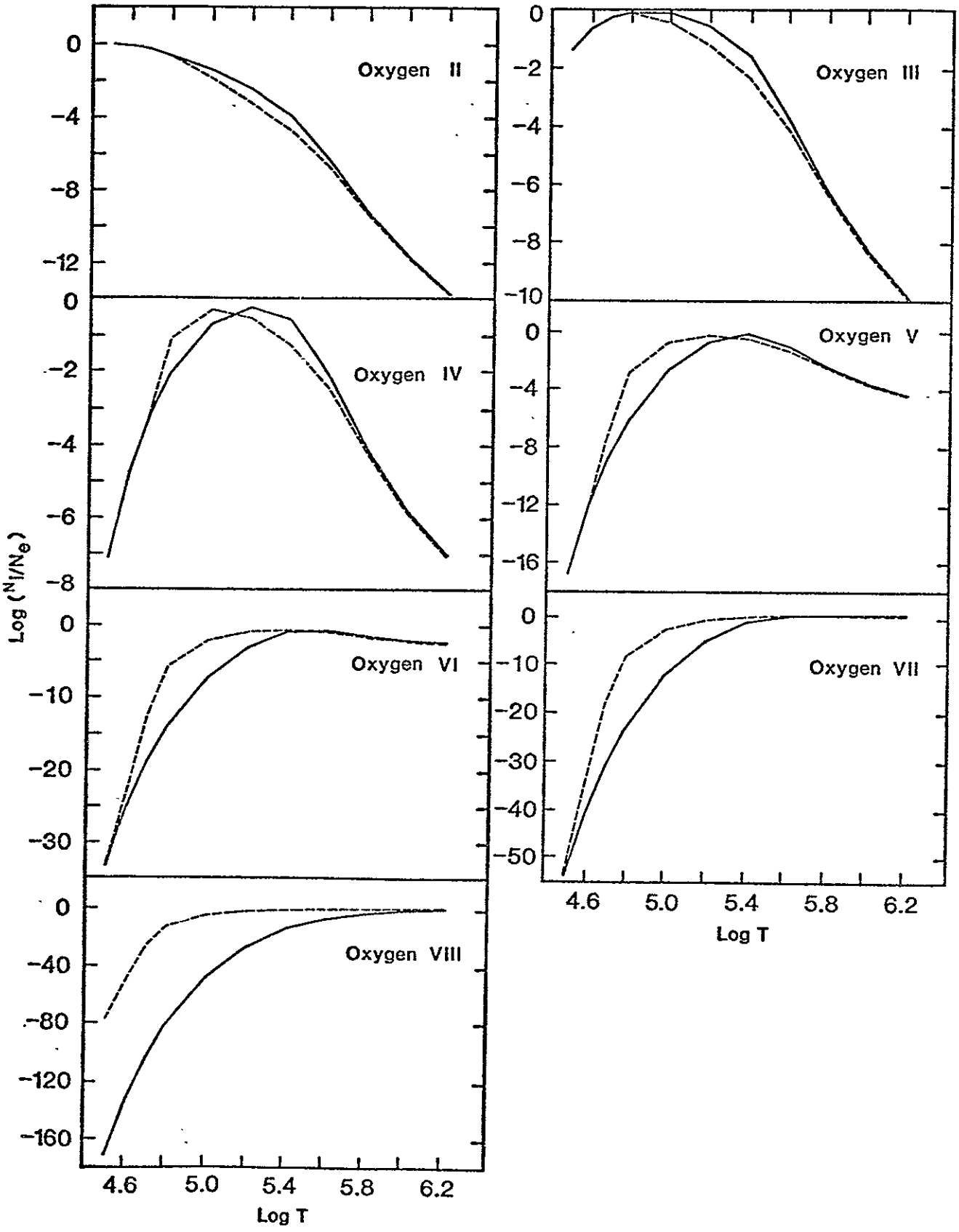
Oxygen II
Oxygen III
Oxygen IV
Oxygen V
Oxygen VI
Oxygen VII
Oxygen VIII
Log (N_i/N_e)
Log T
4.6
5.0
5.4
5.8
6.2

Figure 6

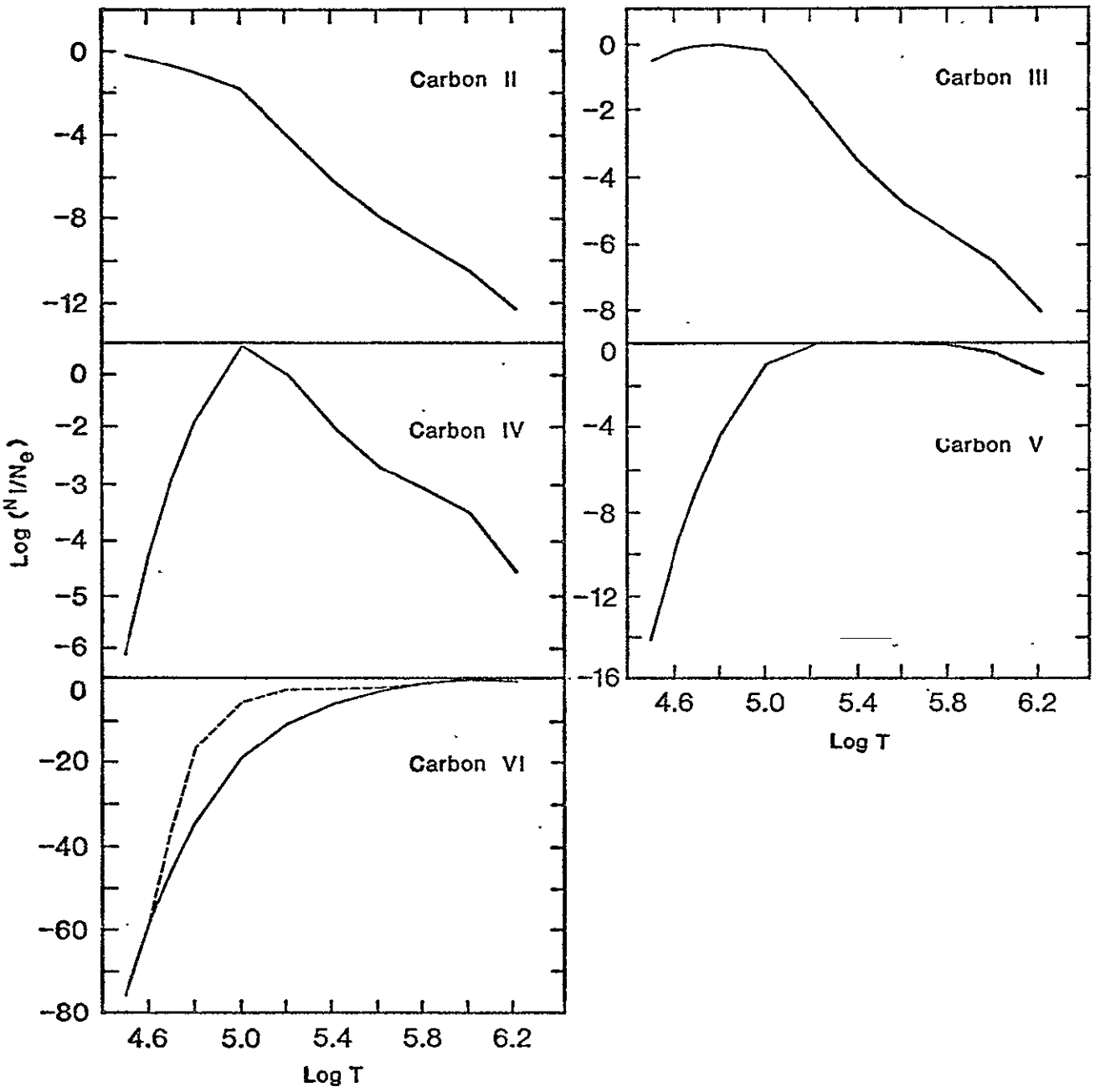
Carbon II
Carbon III
Carbon IV
Carbon V
Carbon VI
Log (N_I/N_e)
Log T
4.6
5.0
5.4
5.8
6.2

Figure 7